Available online at www.sciencedirect.com
ScienceDirect
Journal of Solid State Chemistry 179 (2006) 3751–3755
Journal of Solid State Chemistry
www.elsevier.com/locate/jssc

Thermoelectric properties of p-type pseudo-binary $(Ag_{0.365}Sb_{0.558}Te)_x$–$(Bi_{0.5}Sb_{1.5}Te_3)_{1-x}$ ($x = 0$–1.0) alloys prepared by spark plasma sintering

J.L. Cui[a,*], H.F. Xue[b,a], W.J. Xiu[b,a], L. Jiang[b], P.Z. Ying[b]

[a]School of Mechanical Engineering, Ningbo University of Technology, Ningbo 315016, China
[b]School of Materials Science and Engineering, China University of Mining and Technology, Xuzhou 221008, China

Received 25 April 2006; received in revised form 11 August 2006; accepted 12 August 2006
Available online 17 August 2006

Abstract

In this paper, pseudo-binary $(Ag_{0.365}Sb_{0.558}Te)_x$–$(Bi_{0.5}Sb_{1.5}Te_3)_{1-x}$ ($x = 0$–1.0) alloys were prepared using spark plasma sintering technique, and the composition-dependent thermoelectric properties were evaluated. Electrical conductivities range from 7.9×10^4 to $15.6 \times 10^4\,\Omega^{-1}\,m^{-1}$ at temperatures of 507 and 318 K, respectively, being about 3.0 and 8.5 times those of $Bi_{0.5}Sb_{1.5}Te_3$ alloy at the corresponding temperatures. The optimal dimensionless figure of merit (*ZT*) of the sample with molar fraction $x = 0.025$ reaches 1.1 at 478 K, whereas that of the ternary $Bi_{0.5}Sb_{1.5}Te_3$ alloy is 0.58 near room temperature. The results also reveal that a direct introduction of $Ag_{0.365}Sb_{0.558}Te$ in the Bi–Sb–Te system is much more effective to the property improvement than naturally precipitated $Ag_{0.365}Sb_{0.558}Te$ in the Ag-doped Ag–Bi–Sb–Te system.

Keywords: Pseudo-binary $(Ag_{0.365}Sb_{0.558}Te)_x$–$(Bi_{0.5}Sb_{1.5}Te_3)_{1-x}$ alloys; Spark plasma sintering; Thermoelectric properties

1. Introduction

The thermoelectric efficiency of a material is determined by figure of merit *Z*, which is a combination of three transport quantities: $Z = \alpha^2\sigma/\kappa$, where α is the Seebeck coefficient, σ is the electrical conductivity and κ is the thermal conductivity, which involves both electronic and lattice components $\kappa_{\mathrm{lattice}}$ and κ_L, respectively. A high *Z* value reduces to maximizing the power factor $\alpha^2\sigma$ and minimizing κ. However, attempts over a 40-year period to improve the thermoelectric efficiency of bulk Bi–Te-based room temperature materials, simply prepared using powder metallurgy procedure, have met with limited success, and solid solutions based on Bi_2Te_3 and PbTe still remain the best thermoelectric materials for room and mid-temperature operation.

A broad search has been under way to identify new materials with enhanced thermoelectric properties [1,2]; a group of materials where a higher performance can be expected are alloys such as $(AgSbTe_2)_x$–$(Pb_{0.5}Sn_{0.5}Te)_{1-x}$ [3] and $Ag(Pb_{1-y}Sn_y)_mSbTe_{2+m}$ [4] with the maximum *ZT* values of 1 and 1.45 at 700 and 627 K, respectively, and Ge(Sn,Pb)Te–Bi_2Te_3 [5] and $n\mathrm{GeTe}\cdot m\mathrm{Bi_2Te_3}$ systems [6] with complex structures. Materials with complex structure could expect to exhibit glass-like thermal conductivities. For example, adding other elements to yield four- and five-element compounds can lead to mass-fluctuation scattering of the phonons [7], resulting in reduced lattice thermal conductivity [6,8], thus in effect improving thermoelectric performance.

Results from recent research in our group evidenced that a proper substitution of Cu and Ag atoms for Sb in the $Bi_{0.5}Sb_{1.5}Te_3$ alloy is essential for improving thermoelectric performance [9,10], and the second phase $Ag_{0.365}Sb_{0.558}Te$ naturally precipitated in the Ag-doped $Ag_xBi_{0.5}Sb_{1.5-x}Te_3$ ($x = 0.05$–0.4) alloys [10] was assumed to play an important role in reducing the thermal conductivity at higher temperatures because of lattice distortion. $Ag_{0.365}Sb_{0.558}Te$ is a ternary compound with cubic-type

---

*Corresponding author. Fax: +86 574 8708 1258.
E-mail address: cuijl@nbip.net (J.L. Cui).

0022-4596/$ - see front matter © 2006 Elsevier Inc. All rights reserved.
doi:10.1016/j.jssc.2006.08.016

structure (sp. gr. *Fm-3m*); this precipitated compound in Ag–Bi–Sb–Te systems noticeably alters the temperature dependence of the thermoelectric figure of merit (*ZT*), demonstrating that the maximum *ZT* value shifts to the higher temperature side [10]. However, the clear action and mechanism of $Ag_{0.365}Sb_{0.558}Te$, if it purposely solution-solidifies with another ternary alloy $Bi_{0.5}Sb_{1.5}Te_3$ to form pseudo-binary $(Ag_{0.365}Sb_{0.558}Te)_x$–$(Bi_{0.5}Sb_{1.5}Te_3)_{1-x}$ alloys, has not been experimentally determined yet.

Spark plasma sintering (SPS) is a rapid sintering method for fabricating bulk materials [11]. Due to the application of pulsed DC current between the graphite die and the starting powders, a self-heating is realized for metal or semiconductor materials, and a homogeneous material at a relatively low temperature can possibly be obtained in a much shorter sintering time than the conventional methods. SPS can also provide a potential advantage in fabricating Bi_2Te_3-based materials with low melting point, by suppressing the occurrence of elemental evaporation, such as that of element Te, and grain growth, because of a rapid densification. Small grain size can be beneficial in reducing lattice thermal conductivity.

In the present work, a group of pseudo-binary alloys $(Ag_{0.365}Sb_{0.558}Te)_x$–$(Bi_{0.5}Sb_{1.5}Te_3)_{1-x}$ ($x = 0$–1.0) were prepared by SPS technique, and the effect of the ternary alloy $Ag_{0.365}Sb_{0.558}Te$ on the thermoelectric properties was evaluated.

2. Experimental

Two mixtures, consisting of elements Ag, Bi, Sb and Te with a purity of more than 99.999% in a stoichiometric ratio of compounds $Ag_{0.365}Sb_{0.558}Te$ and $Bi_{0.5}Sb_{1.5}Te_3$, were sealed in two different vacuum quartz tubes and then melted for 10 h at 1323 K, during which 30-s rocking every 1 h was conducted to ensure that the composition was homogeneous without segregation. After quenching, the two ingots $Ag_{0.365}Sb_{0.558}Te$ and $Bi_{0.5}Sb_{1.5}Te_3$ were once more sealed and melted in vacuum tubes according to a stoichiometry of $(Ag_{0.365}Sb_{0.558}Te)_x$–$(Bi_{0.5}Sb_{1.5}Te_3)_{1-x}$ ($x = 0$, 0.025, 0.05, 0.1, 0.2, 0.4,1.0). The obtained $(Ag_{0.365}Sb_{0.558}Te)_x$–$(Bi_{0.5}Sb_{1.5}Te_3)_{1-x}$ ingots with different molar fraction x were ball-milled in stainless steel bowls for 5 h with a rotation rate of 350 rpm. The powders, after drying in vacuum for 5 h at 60 °C, were sintered at 623 K with a pressure of 40 MPa using an SPS apparatus (SPS-1030), and the samples obtained with a size of ϕ 20 mm × 2.5 mm were eventually cut into 3 mm slices measuring 2.5 mm × 15 mm; the densities of the samples were measured by an Archimedes method.

The electrical properties involving Seebeck coefficients (α) and electrical conductivities (σ) were measured using an apparatus (ULVAC ZEM-2) in a helium atmosphere, and thermal diffusivities were measured by a laser flash method (Netzsch, LFA427). Thermal conductivities were calculated from the values of density, specific heats and thermal diffusivities. The structural analyses were directly taken with an X-ray diffractometer (XRD-98) using Cu$K\alpha$ radiation ($\lambda = 0.15406$ nm), using a scan rate of 4° min^{-1} to record patterns in the 2θ range from 10° to 100°. The chemical compositions were analyzed with electron probe microanalysis (EPMA-8705QH2) with an accuracy of more than ±97%.

3. Results and discussion

Densities of the $(Ag_{0.365}Sb_{0.558}Te)_x$–$(Bi_{0.5}Sb_{1.5}Te_3)_{1-x}$ samples ($x = 0.025$–0.4) were measured and range from 6.55×10^3 to 6.63×10^3 kg m^{-3} (see Fig. 1), being a little higher than that of $Bi_{0.5}Sb_{1.5}Te_3$ (6.50×10^3 kg m^{-3}). X-ray diffraction patterns of alloys are given in Fig. 2; patterns (a)–(e) represent compounds belonging to a common

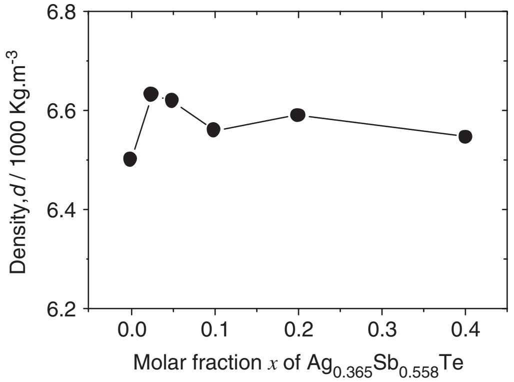

Fig. 1. The relationship between density and molar fraction x for the pseudo-binary $(Ag_{0.365}Sb_{0.558}Te)_x$–$Bi_{0.5}Sb_{1.5}Te_3)_{1-x}$ ($x = 0$–0.4) alloys prepared by spark plasma sintering.

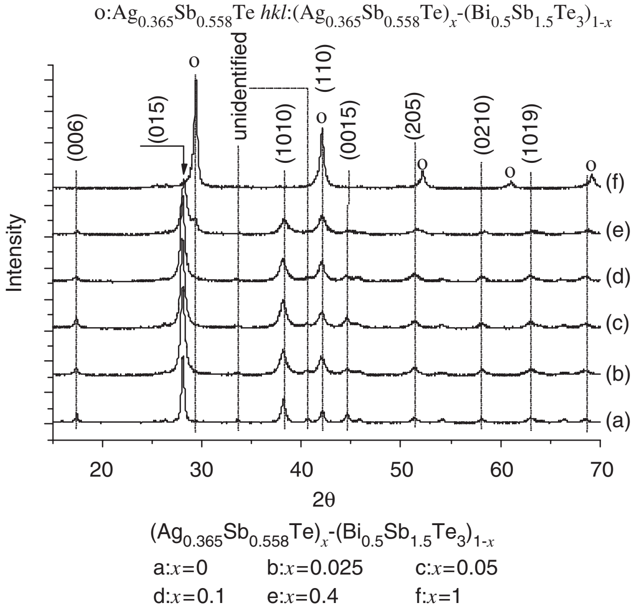

Fig. 2. X-ray diffraction patterns of the $(Ag_{0.365}Sb_{0.558}Te)_x$–$(Bi_{0.5}Sb_{1.5}Te_3)_{1-x}$ ($x = 0$–0.4) alloys: (a) $x = 0$; (b) $x = 0.025$; (c) $x = 0.05$; (d) $x = 0.1$; (e) $x = 0.4$; (f) $Ag_{0.365}Sb_{0.558}Te$.

homologous series $(Ag_{0.365}Sb_{0.558}Te)_x$–$(Bi_{0.5}Sb_{1.5}Te_3)_{1-x}$ with rhombohedral Sb_2Te_3 structure (sp .gr. $R\bar{3}m$). Pattern (f) relating to the ternary $Ag_{0.365}Sb_{0.558}Te$ alloy is specially indicated for comparison. Peak intensities corresponding to 2θ angles of near 29° and 42° generally increase with molar fraction x, while those with respect to the crystal plane (1010) and (205) decrease gradually, and finally disappear in the ternary $Ag_{0.365}Sb_{0.558}Te$ alloy; this variation is in agreement with that of the content of ternary $Ag_{0.365}Sb_{0.558}Te$ alloy in the raw mixtures. Some unidentified phases have been detected with respect to 2θ angles of about 33° and 41°, shown in Fig. 2; these unidentified phases can possibly be oxides since a small amount of oxygen, in addition to four main elements Ag, Sb, Bi, Te, was detected using EPMA, as shown in Table 1, thus to a certain extent influencing thermoelectric properties. The analyzed molar fraction of element Ag gradually increases with molar fraction x in the raw mixtures and that of element Bi is relatively low for the alloy with $x = 0.4$. Through elemental distribution analysis to polished surfaces for samples with $x = 0.025$ and 0.4, we observed no obvious elemental segregation; therefore, we cannot exclude the possibility of the formation of quaternary Ag–Sb–Bi–Te alloys.

The relationships between Seebeck coefficient (α) and temperature are presented in Fig. 3. The $(Ag_{0.365}Sb_{0.558}Te)_x$–$(Bi_{0.5}Sb_{1.5}Te_3)_{1-x}$ alloys show positive α values in the whole temperature region, indicating p-type semiconductor behavior. The α values increase with measuring temperature monotonously; the rising trend is opposite to that of ternary $Bi_{0.5}Sb_{1.5}Te_3$ alloy, which decreases from 272.5 to 101.0 μV/K. The slope of the Seebeck coefficients has completely changed upon adding $Ag_{0.365}Sb_{0.558}Te$, which might pertain to considerable electronic changes at Fermi level. The α value decreases regularly with $Ag_{0.365}Sb_{0.558}Te$ content increasing in the measuring temperature region, the maximum α value reaches 164.0 μV/K for $x = 0.025$ at about 500 K. Below 460 K, the magnitude of the α value for the $Bi_{0.5}Sb_{1.5}Te_3$ alloy is higher than those of $(Ag_{0.365}Sb_{0.558}Te)_x$–$(Bi_{0.5}Sb_{1.5}Te_3)_{1-x}$ alloys. At temperatures higher than 460 K, the α values for $Bi_{0.5}Sb_{1.5}Te_3$ alloy are going to be lower than those of $(Ag_{0.365}Sb_{0.558}Te)_x$–$(Bi_{0.5}Sb_{1.5}Te_3)_{1-x}$ alloy with $x = 0.025$. The more the content of $Ag_{0.365}Sb_{0.558}Te$, the lower the α values of the samples, while the α values for the directly Ag-doped $Ag_xBi_{0.5}Sb_{1.5-x}Te_3$ alloys are almost the same at measuring temperatures [12]. Particularly note the similar temperature dependence of the Seebeck coefficient of the ternary $Ag_{0.365}Sb_{0.558}Te$ alloy; the rising trend of the ternary alloy $Ag_{0.365}Sb_{0.558}Te$ can be considered as being essential to alter the temperature dependence of Seebeck coefficients of the $(Ag_{0.365}Sb_{0.558}Te)_x$–$(Bi_{0.5}Sb_{1.5}Te_3)_{1-x}$ alloys.

Table 1
Average molar fraction of elements in the alloys analyzed by EMPA (four different points were taken when analyzed)

Samples with x element	Molar fraction of elements			
	$x = 0.025$	$x = 0.05$	$x = 0.10$	$x = 0.40$
Ag	0.011	0.012	0.045	0.132
Sb	1.539	1.532	1.455	1.184
Te	2.935	2.869	2.790	2.183
Bi	0.448	0.450	0.422	0.281
Remaining elements	Oxygen			

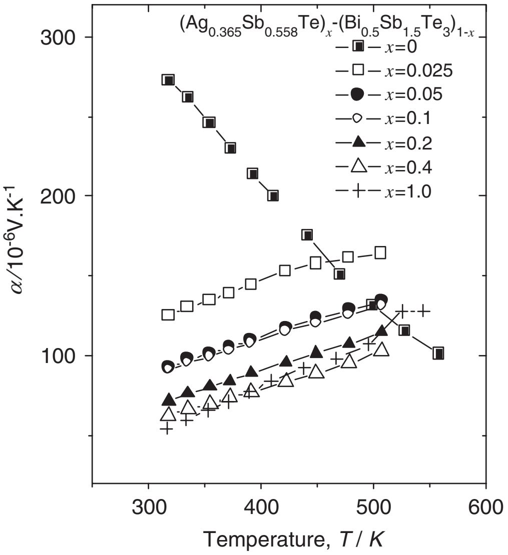

Fig. 3. The relationship between temperature and Seebeck coefficients for the $(Ag_{0.365}Sb_{0.558}Te)_x$–$(Bi_{0.5}Sb_{1.5}Te_3)_{1-x}$ ($x = 0$–1.0) alloys prepared by spark plasma sintering.

The electrical conductivities (σ) against reciprocal temperature are plotted in Fig. 4. It can be seen that all σ values are much higher than those of $Bi_{0.5}Sb_{1.5}Te_3$ alloy; σ values relating to the molar fraction $x = 0.025$ are 7.9×10^4 to $15.6 \times 10^4\,\Omega^{-1}\,m^{-1}$ at temperatures of 507 and 318 K, respectively, being about 3.0 and 8.5 times those of $Bi_{0.5}Sb_{1.5}Te_3$ alloy at corresponding temperatures. The electrical conductivity decreases gradually with measuring temperature for the $(Ag_{0.365}Sb_{0.558}Te)_x$–$(Bi_{0.5}Sb_{1.5}Te_3)_{1-x}$ alloys, but increases mildly with $Ag_{0.365}Sb_{0.558}Te$ content increasing; the maximum σ value of $25.6 \times 10^4\,\Omega^{-1}\,m^{-1}$ can be obtained for $x = 0.4$ at 318 K, and this composition dependence is different from that of directly Ag-doped pseudo-binary $Ag_xBi_{0.5}Sb_{1.5-x}Te_3$ alloys [12]. The ternary alloy $Ag_{0.365}Sb_{0.558}Te$ shows lower σ values than the alloy with $x = 0.4$.

Because the formula of $Ag_{0.365}Sb_{0.558}Te$ can presumably be expressed as $(AgSbTe_2)_{0.365}$–$(Sb_2Te_3)_{0.0965}$, herein the molar ratio of Sb_2Te_3 to $AgSbTe_2$ is about 0.264. This analysis might be reasonable in that it is in good agreement with the fact that $Ag_{0.365}Sb_{0.558}Te$ alloy exhibits cubic structure with $Fm-\bar{3}m$ space group. The compound $Ag_{0.365}Sb_{0.558}Te$ can also be considered as a solid solution of two alloys $AgSbTe_2$ and Sb_2Te_3. We cannot exclude the possible formation of our-layer lamellae of the type

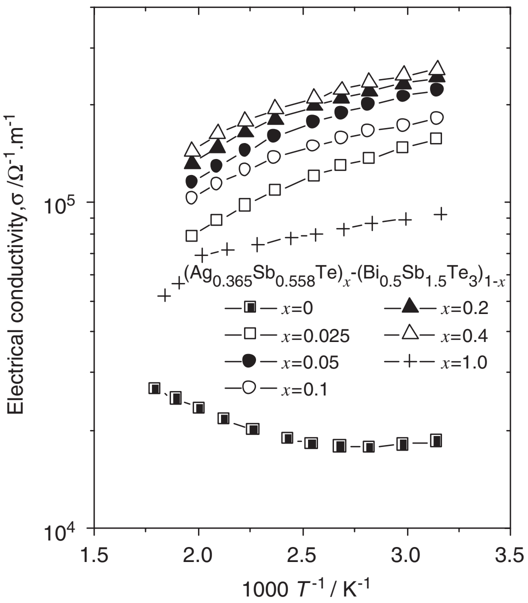

Fig. 4. The dependence of electrical conductivities on temperature for $(Ag_{0.365}Sb_{0.558}Te)_x$–$(Bi_{0.5}Sb_{1.5}Te_3)_{1-x}$ ($x = 0$–1.0) alloys prepared by spark plasma sintering.

$[Ag_{0.5}Sb_{0.5}]$–Te–$[Ag_{0.5}Sb_{0.5}]$–Te, which corresponds to the $AgSbTe_2$ structure, where the crystal planes of the cation sublattice are occupied statistically with Sb and Ag atoms. In comparison with the electrical conductivities of $Bi_{0.5}Sb_{1.5}Te_3$ alloy, and based on the analysis and property evaluation of $Ag_{0.365}Sb_{0.558}Te$ in the present work, it can be estimated that there is another conduction mechanism acting on the $(Ag_{0.365}Sb_{0.558}Te)_x$–$(Bi_{0.5}Sb_{1.5}Te_3)_{1-x}$ alloys. Since the formation of four-layer lamellae within the Sb_2Te_3 structure does not change any charges [13], i.e., carrier concentration n, in this case, a significant improvement of electrical conductivities of $(Ag_{0.365}Sb_{0.558}Te)_x$–$(Bi_{0.5}Sb_{1.5}Te_3)_{1-x}$ alloys are most likely attributed to the enhancement of mobility, μ, according to the expression $\sigma = ne\mu$, where e is electronic charge. Because the $(Ag_{0.365}Sb_{0.558}Te)_x$–$(Bi_{0.5}Sb_{1.5}Te_3)_{1-x}$ alloys possess the same rhombohedral structure (sp. gr. $R\bar{3}m$) as Sb_2Te_3, a special composite, possibly formed and combined four-layer lamellae $[Ag_{0.5}Sb_{0.5}]$–Te–$[Ag_{0.5}Sb_{0.5}]$–Te with Sb_2Te_3 or Bi_2Te_3 slabs with different crystal lattices, might act to favor carrier transportation, thus improving the electrical conductivities of $(Ag_{0.365}Sb_{0.558}Te)_x$–$(Bi_{0.5}Sb_{1.5}Te_3)_{1-x}$ alloys. However, this analysis is not in good agreement well with that in [12], where we analyzed that the main reason to increase the electrical conductivities of Ag-doped $Ag_xBi_{0.5}Sb_{1.5-x}Te_3$ alloys is the enhancement of carrier concentration n. Moreover, Ag^+ and Sb^{3+} might exist in the $AgSbTe_2$ lattice in order to get electroneutrality, which can generate local distortions, both structural and electronic, that are also critical in determining the electrical properties of $(Ag_{0.365}Sb_{0.558}Te)_x$–$(Bi_{0.5}Sb_{1.5}Te_3)_{1-x}$ alloys. However, these explanations require further confirmation.

The total thermal conductivities of $(Ag_{0.365}Sb_{0.558}Te)_x$–$(Bi_{0.5}Sb_{1.5}Te_3)_{1-x}$ alloys are shown over a wide temperature range (Fig. 5a) and increase from 1.21 to 1.82 $W\,K^{-1}\,m^{-1}$ when x increases from 0.025 to 0.4 at near room temperature, respectively. The κ values for the $(Ag_{0.365}Sb_{0.558}Te)_x$–$(Bi_{0.5}Sb_{1.5}Te_3)_{1-x}$ alloys and $Ag_{0.365}Sb_{0.558}Te$ are higher than that of the ternary $Bi_{0.5}Sb_{1.5}Te_3$ alloy at 318 K and show a decreasing trend with temperature. Noting this, relatively stable electronic components $\kappa_{carrier}$ values, calculated according to $\kappa_{carrier} = L\sigma T$, where L is a Lorentz constant ($L = 1.5 \times 10^{-8}\,V^2\,K^{-2}$) [14], and T is absolute temperature, are obtained in the measuring temperature region (Fig. 5b), hence suggesting that it is the lattice component κ_L (see inset in Fig. 5b) that determines the temperature dependence of the total κ. A possible explanation for the decreasing trend of κ_L values with temperature results directly from enhanced phonon scattering. As was discussed above, the four-layer lamellae structure $[Ag_{0.5}Sb_{0.5}]$–Te–$[Ag_{0.5}Sb_{0.5}]$–Te combined possibly with Sb_2Te_3 or Bi_2Te_3 can distort the rhombohedral structure. With the temperature elevation, local distortions produced by charge imbalance of Ag^+ and Sb^{3+} in the $AgSbTe_2$ lattice could also scatter phonons; hence κ_L shows a decreasing trend with rising temperature in the $(Ag_{0.365}Sb_{0.558}Te)_x$–$(Bi_{0.5}Sb_{1.5}Te_3)_{1-x}$ alloys. Another explanation might be due to the formation of Bi_2O_3 and TeO_2 [15]; herein a small amount of oxygen is possibly introduced from the ball milling and incomplete evacuation during quartz tube sealing, as was discussed in [10], although we have not been able to identify these impurities using XRD analysis. These oxides could also reduce the lattice component κ_L and increase the electrical resistivities; however, quantitative results with respect to the influence of Bi_2O_3 and TeO_2 have not been obtained yet.

Fig. 6 indicates the temperature dependence of the thermoelectric figure of merit (ZT). The ZT values increase with measuring temperature for the $(Ag_{0.365}Sb_{0.558}Te)_x$–$(Bi_{0.5}Sb_{1.5}Te_3)_{1-x}$ alloys, and range from 0.64 to 1.1 for the alloy with $x = 0.025$ when temperature was elevated from 318 to 478 K; the rising trend is similar to that of ternary $Ag_{0.365}Sb_{0.558}Te$ alloy. The ZT value of the ternary $Bi_{0.5}Sb_{1.5}Te_3$ alloy is 0.58 at 318 K, showing a decreasing trend with temperature. The ZT value decreases with molar fraction x, which is directly caused by the low Seebeck coefficient and the high κ value at higher concentration of $Ag_{0.365}Sb_{0.558}Te$. If compared with the ZT values in [10], we observe in the present work that the highest ZT value of 1.1 for the alloy with $x = 0.025$ appears at a temperature of 478 K, approximately 80 K lower than that in [10] for the $Ag_xBi_{0.5}Sb_{1-x}Te_3$ alloy with $x = 0.4$, suggesting that a direct introduction of $Ag_{0.365}Sb_{0.558}Te$ in the Bi–Sb–Te system can not only decrease the temperature at which the maximum ZT value reaches, but also reduce the Ag concentration in the alloys, and is much more effective in property improvement than naturally precipitated

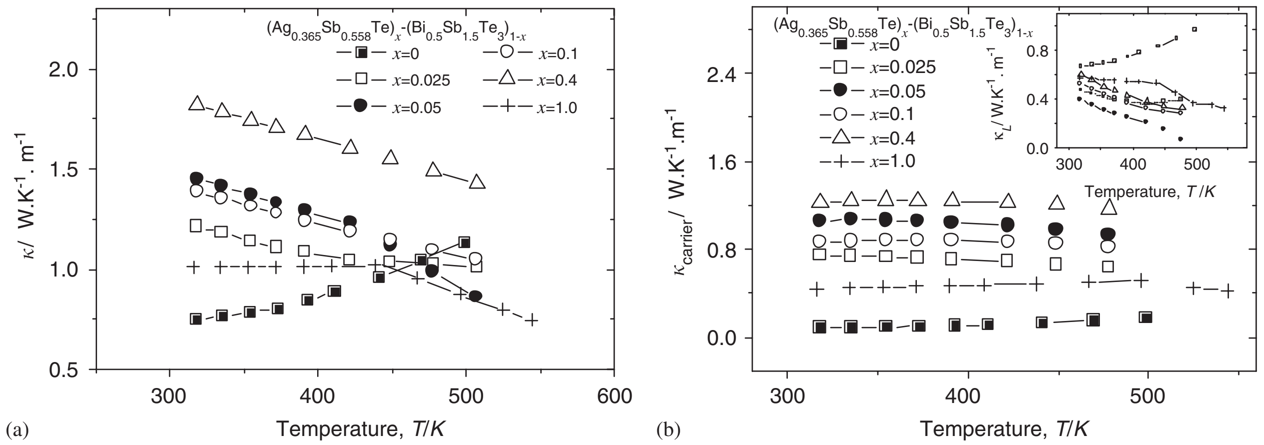

Fig. 5. The temperature dependence of thermal conductivities for different $(Ag_{0.365}Sb_{0.558}Te)_x$–$(Bi_{0.5}Sb_{1.5}Te_3)_{1-x}$ ($x = 0$–1.0) alloys prepared by spark plasma sintering: (a) κ -T; (b) $\kappa_{carrier}$–T (temperature dependence of lattice components κ_L are shown as an inset).

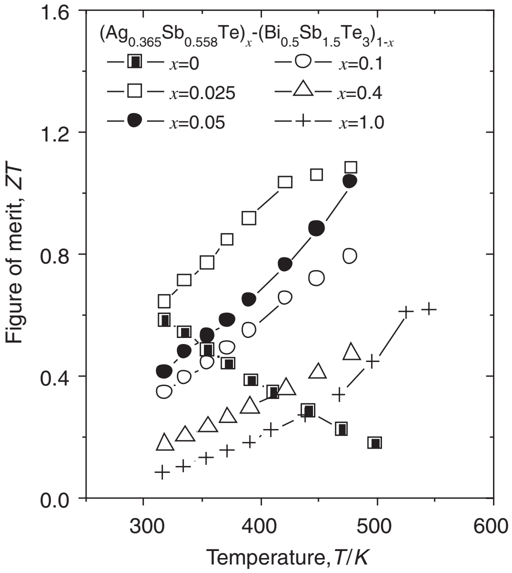

Fig. 6. The temperature dependence of dimensionless thermoelectric figure of merit ZT for different $(Ag_{0.365}Sb_{0.558}Te)_x$-$(Bi_{0.5}Sb_{1.5}Te_3)_{1-x}$ ($x = 0$–1.0) alloys prepared by spark plasma sintering.

$Ag_{0.365}Sb_{0.558}Te$ in the Ag-doped quaternary Ag–Bi–Sb–Te system [10].

4. Conclusions

By applying SPS technique, the pseudo-binary $(Ag_{0.365}Sb_{0.558}Te)_x$–$(Bi_{0.5}Sb_{1.5}Te_3)_{1-x}$ alloys prepared exhibit superior thermoelectric performance in comparison to the ternary $Bi_{0.5}Sb_{1.5}Te_3$ alloy. With $x = 0.025$, the electrical conductivities range from 7.9×10^4 to $15.6 \times 10^4\,\Omega^{-1}\,m^{-1}$ at temperatures of 507 and 318 K, respectively, being about 3.0 and 8.5 times those of $Bi_{0.5}Sb_{1.5}Te_3$ alloy at the corresponding temperatures, and the maximum ZT value of 1.1 is achieved at 478 K, while that of the ternary $Bi_{0.5}Sb_{1.5}Te_3$ alloy is only 0.58 near room temperature. The results reveal that a direct introduction of $Ag_{0.365}Sb_{0.558}Te$ in the Bi–Sb–Te system is much more effective in property improvement than naturally precipitated $Ag_{0.365}Sb_{0.558}Te$ in the Ag-doped Ag–Bi–Sb–Te system.

Acknowledgments

The project was supported by Zhejiang Provincial Natural Science Foundation of China (No. Y404321) and Ningbo Natural Science Foundation of China (No. 2006A610058).

References

[1] K.F. Hsu, S. Loo, F. Guo, W. Chen, J.S. Dyck, C. Uher, T. Hogen, E.K. Polychroniadis, M.G. Kanatzidis, Science 303 (2004) 818–821.
[2] D.Y. Chung, T. Hogen, P. Brazis, M. Rocci-Lane, C. Kannewurf, M. Bastea, C. Uher, M.G. Kanatzidis, Science 287 (2000) 1024–1027.
[3] A. Kosuga, K. Kurosaki, H. Muta, S. Yamanaka, J. Alloys Compds. 416 (2006) 218–221.
[4] J. Androulakis, K.F. Hsu, R. Pcionek, H. Kong, C. Uher, J.J. D'Angelo, A. Downey, T. Hogen, M.G. Kanaztidis, Adv. Mater. 18 (2006) 1170–1173.
[5] L.A. Kuznetsova, V.L. Kuznetsov, D.M. Rowe, J. Phys. Chem. Solids 61 (2000) 1269–1274.
[6] L.E. Shelimova, P.P. Konstantinov, O.G. Karpinsky, E.S. Avilov, M.A. Kretova, V.S. Zemskov, Inorg. Mater. J. Alloys Compds. 329 (2001) 50–62.
[7] T.M. Tritt, Science 283 (1999) 804–805.
[8] L.E. Shelimova, O.G. Karpinskii, P.P. Konstantinov, M.A. Kretova, E.S. Avilov, V.S. Zemskov, Inorg. Mater. 38 (2002) 790–794.
[9] J.L. Cui, J. Alloys Compds. 415 (2006) 216–219.
[10] J.L. Cui, H.F. Xue, W.J. Xiu, Mater. Lett, in press.
[11] M. Omori, Mater. Sci. Eng. A 287 (2000) 183–188.
[12] J.L. Cui, X.B. Xu, Mater. Lett. 59 (2005) 3205–3208.
[13] J. Navrátil, I. Klichová, S. Karamazov, J. Šrámková, J. Horák, J. Solid State Chem. 140 (1998) 29–37.
[14] R. Venkatasubramanian, E. Siivola, T. Colpitts, B. O'Quinn, Nature 413 (2001) 597–602.
[15] H. Bando, K. Koizumi, K. Daikohara, Y. Oikawa, V.A. Kulbachinskii, H. Ozaki, in: Proceedings of the 18th International Conference on Thermoelectrics, Baltimore, MD, USA, ICT, 1999, IEEE Catalog No.99TH8407, 1999, p. 359.